IEEE Access
Multidisciplinary | Rapid Review | Open Access Journal

Received January 20, 2020, accepted February 22, 2020, date of publication March 3, 2020, date of current version March 13, 2020.

Digital Object Identifier 10.1109/ACCESS.2020.2977978

Accurate Frequency Estimator of Sinusoid Based on Interpolation of FFT and DTFT

LEI FAN[1], GUOQING QI[2], JUN XING[1], JIYU JIN[1], JINYU LIU[1], AND ZHISEN WANG[1]
[1]School of Information Science and Engineering, Dalian Polytechnic University, Dalian 116034, China
[2]College of Information Science and Technology, Dalian Maritime University, Dalian 116026, China

Corresponding author: Guoqing Qi (qgq@dlmu.edu.cn)

This work was supported by the Provincial Natural Science Foundation Guidance Plan of China under Grant 2019-ZD-0294.

ABSTRACT An accurate frequency estimator of complex sinusoid in additive white noise is proposed. It is based on interpolation of Fast Fourier Transform (FFT) and Discrete-Time Fourier Transform (DTFT). Zero-padding is firstly performed before the FFT of the sinusoid sampled data, and the coarse estimate is obtained by searching the discrete frequency index of the maximum FFT spectrum line. Then the fine estimate is obtained by employing the maximum FFT spectrum line and two DTFT sample values located on the left and right side of the maximum spectrum line. The correlation coefficients between the Fourier Transform of the noises on two arbitrarily spaced spectrum lines are derived, and the MSE calculation formula is derived in additive white noise background based on the correlation coefficients. Simulations results demonstrate that the proposed algorithm has lower MSE than the competing algorithms, and its signal-to-noise ratio (SNR) threshold is lower compared with Candan algorithm, AM algorithm and Djukanovic algorithms.

INDEX TERMS Frequency estimation, FFT, DTFT, interpolation.

I. INTRODUCTION

Sinusoidal frequency estimation can be applied in numerous fields such as radar, sonar, measurement, instrumentation, power systems, communications and so on. Many sinusoidal frequency estimators have been proposed and they can be categorized into time-domain estimators [1]–[3] and frequency-domain estimators [4]–[28]. Time-domain estimators generally have low computational efficiency, and are not appropriate to be used in real-time applications. On the other hand, frequency-domain estimators based on FFT have the advantage of high computation speed and can easily be realized in hardware.

The sinusoidal frequency can be described as $f_0 = (m + \delta)\Delta f$, where m is the index of the peak magnitude of FFT, and δ is the residual frequency with the value range of $[-0.5, 0.5]$. Δf is the FFT frequency resolution. The FFT based sinusoidal frequency estimators can usually be carried out in two stages. Firstly, the coarse estimate is obtained by searching the discrete frequency index of the maximum FFT spectrum line. Next, the fine estimate is usually obtained by interpolation with the maximum FFT spectrum line and the neighboring spectrum lines.

The associate editor coordinating the review of this manuscript and approving it for publication was Yue Zhang.

The maximum likelihood (ML) method produces the least MSE [1] at the cost of low computational efficiency. The maximum FFT spectrum line and the second largest spectrum line are utilized to perform frequency estimation [4], [5]. But when the signal frequency is close to an integral multiple of Δf, the estimation error increases obviously. In consideration of the above disadvantage of frequency interpolation with two FFT spectrum lines, different improved methods have been proposed [6]–[12]. Three samples around the peak in the FFT spectrum are utilized for the frequency estimation [6], [7]. Zero-padding is carried out before the FFT of the sinusoid sampled data, and the two neighboring spectrum line of the maximum FFT spectrum line are used for the fine estimation [8]. RCTSL estimator [9] utilizes three samples around the peak in the $2N$-point FFT spectrum to get the fine estimate. AM estimator [10] makes use of the two DFT samples located on the left and right side of the maximum FFT spectrum line, and its estimation variance is very close to the Cramer-Rao lower bound (CRLB) after two iterations. Based on the best linear unbiased estimation fusion rule, all the spectrum lines can be used for the fine estimation [12], and the precision after iterations is similar to that of the estimator in [10]. When there are interfering signals, windowing methods can be utilized [20]–[28]. The estimation expression of Candan estimator [6] is generalized in [20] when window functions are adopted. When generic cosine

windows are used, Candan method [6] and AM method [10] are generalized in [21].

An accurate sinusoidal frequency estimation algorithm based on interpolation of FFT and DTFT is proposed in this paper. Zero-padding is performed before the FFT of the sinusoid sampled data. The coarse estimate is obtained by finding the discrete frequency index of the maximum FFT spectrum line. The fine estimate is obtained by employing the maximum FFT spectrum line and two DTFT sample values of the sinusoid located on the left and right side of the maximum FFT spectrum line. These two DTFT sample values are closer to the DTFT peak of the sinusoid than the spectrum lines used by the estimators in [6]–[10]. Therefore, these two DTFT sample values utilized by the proposed estimator are less affected by the noise, and the proposed estimator should outperform the existing estimators in [6]–[10] in additive white noise. As the intervals between the spectrum lines utilized by the proposed algorithm are smaller than Δf which is the frequency resolution of N-point FFT, the noise on these spectrum lines are correlated. The correlation coefficients between the Fourier Transform of the noises on two arbitrarily spaced spectrum lines are derived. With these correlation coefficients, the MSE calculation formula is derived in additive white noise. Simulations are performed, and the results demonstrate that the proposed algorithm has lower MSE than the competing algorithms, and its signal-to-noise ratio (SNR) threshold is lower compared with Candan algorithm [6], AM algorithm [10], Djukanovic algorithms [13], [14].

The rest of the work is structured as follows. In Section II, the estimation expression is derived and the iterative procedures are described. In Section III, the MSE calculation formula is derived. In section IV, the MSE calculation formula and the performance of the proposed estimator are verified through simulations. Finally, Section V concludes the work.

II. PROPOSED ALGORITHM

The signal can be expressed as [11]:

$$x(n) = s(n) + z(n), \quad n = 0, 1, \ldots, N-1 \tag{1}$$

$$s(n) = A\mathrm{e}^{\mathrm{j}(2\pi fn/f_s+\varphi)}, \quad n = 0, 1, \ldots, N-1 \tag{2}$$

where the complex white noise term $z(n)$ has zero mean and its variance is σ^2. A is the amplitude, f is the frequency and φ is the initial phase. f_s is the frequency of sampling. N is the samples number. The SNR can be defined as $SNR = A^2/\sigma^2$.

Pad N zeros to $s(n)$, $s'(n)$ is obtained. The $2N$-point FFT of $s'(n)$ in a noiseless case is

$$\begin{aligned} S(k) &= \sum_{n=0}^{N-1} A\mathrm{e}^{\mathrm{j}\phi}\mathrm{e}^{\mathrm{j}2\pi\frac{f}{f_s}n}\mathrm{e}^{-\mathrm{j}\frac{\pi}{N}nk} \\ &= A\mathrm{e}^{\mathrm{j}\phi}\mathrm{e}^{\mathrm{j}\pi(N-1)\left(\frac{f}{f_s}-\frac{k}{2N}\right)}\frac{\sin\left[\pi N\left(\frac{f}{f_s}-\frac{k}{2N}\right)\right]}{\sin\left[\pi\left(\frac{f}{f_s}-\frac{k}{2N}\right)\right]}, \\ & \quad k = 0, 1, \ldots, 2N-1 \end{aligned} \tag{3}$$

The coarse estimate is obtained by finding the discrete frequency index of the maximum FFT spectrum line which is denoted as m. And the coarse estimate is $m\Delta f$, where $\Delta f = f_s/(2N)$ is the FFT frequency resolution.

The complex values of the maximum FFT spectrum line and two DTFT sample values of $s'(n)$ at the location $f = (m \pm 0.5)\Delta f$ are utilized to get the fine estimate. These two DTFT sample values are closer to the DTFT peak of the signal than the spectrum lines utilized by the estimators in [6]–[10].

At the location $f = (m+p)\Delta f$, the DTFT sample value of $s'(n)$ is

$$S_p = \sum_{n=0}^{N-1} s(n)\mathrm{e}^{-j2\pi fn}|_{f=(m+p)\Delta f} \tag{4}$$

By substituting $f = (m+\delta)f_s/(2N)$ into (3), formula (4) can be expressed as

$$S_p = \frac{A\mathrm{e}^{\mathrm{j}\varphi}}{2N} \cdot \frac{1-\mathrm{e}^{\mathrm{j}\pi(\delta-p)}}{1-\mathrm{e}^{\mathrm{j}\pi(\delta-p)/N}} \tag{5}$$

When $N \gg \pi(\delta - p)$, $e^{\mathrm{j}\pi(\delta-p)/\mathrm{N}} \approx 1 + \mathrm{j}\pi(\delta - p)/\mathrm{N}$. Formula (4) can be expressed as

$$S_p = \frac{b_p}{\delta - p} \tag{6}$$

where

$$b_p = \frac{\mathrm{j}A\mathrm{e}^{\mathrm{j}\varphi}}{2\pi}\left[1-\mathrm{e}^{\mathrm{j}\pi(\delta-p)}\right] \tag{7}$$

In (6) and (7), let p equal to 0, 0.5 and -0.5 respectively. After some deduction, the following expressions are obtained

$$\frac{S_{-0.5}}{S_0}\left(1+\frac{0.5}{\delta}\right) - 1 = \mathrm{e}^{\mathrm{j}\pi\delta}\left[\frac{S_{-0.5}}{S_0}\left(1+\frac{0.5}{\delta}\right) - \mathrm{j}\right] \tag{8}$$

$$\frac{S_{0.5}}{S_0}\left(1-\frac{0.5}{\delta}\right) - 1 = \mathrm{e}^{\mathrm{j}\pi\delta}\left[\frac{S_{0.5}}{S_0}\left(1-\frac{0.5}{\delta}\right) + \mathrm{j}\right] \tag{9}$$

After some deduction with (8) and (9), δ can be estimated as follows:

$$\hat{\delta} = \mathrm{Re}\left\{\frac{0.5\left[(1-\mathrm{j})S_{0.5} + (1+\mathrm{j})S_{-0.5}\right]}{(1-\mathrm{j})S_{0.5} + 2\mathrm{j}S_0 - (1+\mathrm{j})S_{-0.5}}\right\} \tag{10}$$

where the real part of the expression is taken in order to obtain a real-valued estimate of δ in the noise background.

The sinusoidal frequency is

$$\hat{f} = (m + \hat{\delta}) \cdot \Delta f \tag{11}$$

Inspired by the literature [10], the frequency can be estimated in an iterative manner to further improve the estimation performance. The iterative procedures are shown as follows.

III. THEORETICAL ANALYSIS

The $2N$-point DFT of is as follows:

$$X(k) = S(k) + Z(k), \quad k = 0, 1, 2, \ldots\ldots N-1 \tag{12}$$

At the maximum spectrum line location, $X(k)$ can be expressed as

$$X_0 = S_0 + Z_0 \tag{13}$$

TABLE 1. Iterative procedures of the estimator.

Step	Description
1	Set $\hat{\delta} \leftarrow 0$
2	Pad N zeros to $s(n)$, perform $2N$-point FFT of $s'(n)$, then search m
3	Compute $S_{0.5}$ and $S_{-0.5}$ via (4)
4	Generate $\hat{\delta}_1$ with S_0, $S_{0.5}$ and $S_{-0.5}$ via (10)
5	Set $\hat{\delta} \leftarrow \hat{\delta} + \hat{\delta}_1$
6	If $\hat{\delta}_1$ is small enough,
7	Go to Step 13
8	Else,
9	Compute $S_{\hat{\delta}_1}$, $S_{\hat{\delta}_1+0.5}$ and $S_{\hat{\delta}_1-0.5}$ via (4)
10	Generate $\hat{\delta}_1$ with $S_{\hat{\delta}_1}$, $S_{\hat{\delta}_1+0.5}$ and $S_{\hat{\delta}_1-0.5}$ via (10)
11	Go to Step 5
12	End of If
13	Finally $\hat{f} = (m + \hat{\delta}) \cdot \Delta f$

The two DTFT sample values of $s'(n)$ at the location $f = (m \pm 0.5)\Delta f$ are as follows:

$$X_{0.5} = S_{0.5} + Z_{0.5} \tag{14}$$

$$X_{-0.5} = S_{-0.5} + Z_{-0.5} \tag{15}$$

Replace S_0, $S_{0.5}$ and $S_{-0.5}$ in (10) with X_0, $X_{0.5}$ and $X_{-0.5}$ respectively, then $\hat{\delta}$ can be expressed as

$$\begin{aligned}
&\hat{\delta} \\
&= \frac{0.5[(1-\mathrm{j})X_{0.5} + (1+\mathrm{j})X_{-0.5}]}{(1-\mathrm{j})X_{0.5} - (1+\mathrm{j})X_{-0.5} + 2\mathrm{j}X_0} \\
&= \frac{0.5[(1-\mathrm{j})S_{0.5} + (1-\mathrm{j})Z_{0.5} + (1+\mathrm{j})S_{-0.5} + (1+\mathrm{j})Z_{-0.5}]}{(1-\mathrm{j})S_{0.5} - (1+\mathrm{j})S_{-0.5} + 2\mathrm{j}S_0 + (1-\mathrm{j})Z_{0.5} - (1+\mathrm{j})Z_{-0.5} + 2\mathrm{j}Z_0} \\
&= \frac{0.5[(1-\mathrm{j})S_{0.5} + (1+\mathrm{j})S_{-0.5} + (1-\mathrm{j})Z_{0.5} + (1+\mathrm{j})Z_{-0.5}]}{1 + \frac{(1-\mathrm{j})Z_{0.5} - (1+\mathrm{j})Z_{-0.5} + 2\mathrm{j}Z_0}{(1-\mathrm{j})S_{0.5} - (1+\mathrm{j})S_{-0.5} + 2\mathrm{j}S_0}} \\
&\quad \cdot \frac{1}{(1-\mathrm{j})S_{0.5} - (1+\mathrm{j})S_{-0.5} + 2\mathrm{j}S_0}
\end{aligned} \tag{16}$$

Under high *SNR*, the following expression is obtained

$$\begin{aligned}
&\left[(1-\mathrm{j})Z_{0.5} - (1+\mathrm{j})Z_{-0.5} + 2\mathrm{j}Z_0\right] \\
&\qquad \ll \left[(1-\mathrm{j})S_{0.5} - (1+\mathrm{j})S_{-0.5} + 2\mathrm{j}S_0\right]
\end{aligned} \tag{17}$$

Then a first order Taylor series expansion of (16) is made. And (16) can be expressed as

$$\begin{aligned}
&\hat{\delta} \\
&= \frac{0.5\left[(1-\mathrm{j})S_{0.5} + (1+\mathrm{j})S_{-0.5} + (1-\mathrm{j})Z_{0.5} + (1+\mathrm{j})Z_{-0.5}\right]}{(1-\mathrm{j})S_{0.5} - (1+\mathrm{j})S_{-0.5} + 2\mathrm{j}S_0} \\
&\quad \cdot \left[1 - \frac{(1-\mathrm{j})Z_{0.5} - (1+\mathrm{j})Z_{-0.5} + 2\mathrm{j}Z_0}{(1-\mathrm{j})S_{0.5} - (1+\mathrm{j})S_{-0.5} + 2\mathrm{j}S_0}\right] \\
&\approx \frac{0.5\left[(1-\mathrm{j})S_{0.5} + (1+\mathrm{j})S_{-0.5}\right]}{(1-\mathrm{j})S_{0.5} - (1+\mathrm{j})S_{-0.5} + 2\mathrm{j}S_0} + \frac{0.5\left[(1-\mathrm{j})Z_{0.5} + (1+\mathrm{j})Z_{-0.5}\right]}{(1-\mathrm{j})S_{0.5} - (1+\mathrm{j})S_{-0.5} + 2\mathrm{j}S_0} \\
&\quad - \frac{\left[(1-\mathrm{j})S_{0.5} + (1+\mathrm{j})S_{-0.5}\right]\left[(1-\mathrm{j})Z_{0.5} - (1+\mathrm{j})Z_{-0.5} + 2\mathrm{j}Z_0\right]}{2\left[(1-\mathrm{j})S_{0.5} - (1+\mathrm{j})S_{-0.5} + 2\mathrm{j}S_0\right]^2}
\end{aligned} \tag{18}$$

In the last step of (18), the assumption that $\left[(1-\mathrm{j})Z_{0.5} + (1+\mathrm{j})Z_{-0.5}\right] \ll \left[(1-\mathrm{j})S_{0.5} + (1+\mathrm{j})S_{-0.5}\right]$ under high *SNR* is used. Under the noiseless circumstance, the estimate of δ is close to the true value. So the following expression is obtained

$$\frac{0.5[(1-\mathrm{j})S_{0.5} + (1+\mathrm{j})S_{-0.5}]}{(1-\mathrm{j})S_{0.5} - (1+\mathrm{j})S_{-0.5} + 2\mathrm{j}S_0} \approx \delta \tag{19}$$

Substituting (19) into (18), (18) can be expressed as

$$\begin{aligned}
\hat{\delta} \approx \delta &+ \frac{0.5\left[(1-\mathrm{j})Z_{0.5} + (1+\mathrm{j})Z_{-0.5}\right]}{(1-\mathrm{j})S_{0.5} - (1+\mathrm{j})S_{-0.5} + 2\mathrm{j}S_0} \\
&- \delta \cdot \frac{\left[(1-\mathrm{j})Z_{0.5} - (1+\mathrm{j})Z_{-0.5} + 2\mathrm{j}Z_0\right]}{\left[(1-\mathrm{j})S_{0.5} - (1+\mathrm{j})S_{-0.5} + 2\mathrm{j}S_0\right]}
\end{aligned} \tag{20}$$

After simple algebra, the following expression is obtained

$$\hat{\delta} - \delta \approx \frac{\left[(1-\mathrm{j})(0.5-\delta)Z_{0.5} + (1+\mathrm{j})(0.5+\delta)Z_{-0.5} - 2\mathrm{j}\delta Z_0\right]}{(1-\mathrm{j})S_{0.5} - (1+\mathrm{j})S_{-0.5} + 2\mathrm{j}S_0} \tag{21}$$

Since the mean values of Z_0, $Z_{0.5}$ and $Z_{-0.5}$ are all zero, it can be concluded that $E\left(\hat{\delta}\right) \approx E\left(\delta\right)$. Therefore,$\hat{\delta}$ is the unbiased estimate of δ.

The expression on the left of (21) is real-valued. Therefore, the real part of the expression on the right of (21) is taken in order to obtain a real-valued result as follows:

$$\hat{\delta} - \delta \approx \mathrm{Re}\left\{\frac{\left[(1-\mathrm{j})(0.5-\delta)Z_{0.5} + (1+\mathrm{j})(0.5+\delta)Z_{-0.5} - 2\mathrm{j}\delta Z_0\right]}{(1-\mathrm{j})S_{0.5} - (1+\mathrm{j})S_{-0.5} + 2\mathrm{j}S_0}\right\} \tag{22}$$

The MSE of the estimate of δ is

$$\begin{aligned}
&E\left[\left(\hat{\delta} - \delta\right)^2\right] \\
&\approx E\left[\left(\mathrm{Re}\left\{\frac{(1-\mathrm{j})(0.5-\delta)Z_{0.5} + (1+\mathrm{j})(0.5+\delta)Z_{-0.5} - 2\mathrm{j}\delta Z_0}{(1-\mathrm{j})S_{0.5} - (1+\mathrm{j})S_{-0.5} + 2\mathrm{j}S_0}\right\}\right)^2\right]
\end{aligned} \tag{23}$$

In order to obtain the formula of $E\left[\left(\hat{\delta} - \delta\right)^2\right]$, the denominator of (22) is considered first. According to the definition of DTFT, the following expression is obtained

$$S\left(m+i\right) = A\mathrm{e}^{\mathrm{j}\phi}\mathrm{e}^{\mathrm{j}\pi\left(\frac{N-1}{2N}\right)(\delta-i)}\frac{\sin\left[\frac{\pi}{2}(\delta-i)\right]}{\sin\left[\frac{\pi}{2N}(\delta-i)\right]} \tag{24}$$

When N is large, (24) can be expressed as

$$S\left(m+i\right) \approx A\mathrm{e}^{\mathrm{j}\phi}\mathrm{e}^{\mathrm{j}\frac{\pi}{2}(\delta-i)}\frac{2N\sin\left[\frac{\pi}{2}(\delta-i)\right]}{\pi(\delta-i)} \tag{25}$$

Let i equals to 0, 0.5 and -0.5 respectively, the following expressions are obtained

$$S_0 \approx \mathrm{e}^{\mathrm{j}\phi}\mathrm{e}^{\mathrm{j}\frac{\pi}{2}\delta} \cdot \frac{2AN\sin\left(\frac{\pi}{2}\delta\right)}{\pi\delta} \tag{26}$$

$$S_{0.5} \approx \mathrm{e}^{\mathrm{j}\phi}\mathrm{e}^{\mathrm{j}\frac{\pi}{2}\left(\delta-\frac{1}{2}\right)} \cdot \frac{2AN\sin\left[\frac{\pi}{2}(\delta-0.5)\right]}{\pi(\delta-0.5)} \tag{27}$$

$$S_{-0.5} \approx e^{j\phi} e^{j\frac{\pi}{2}(\delta+\frac{1}{2})} \cdot \frac{2AN \sin\left[\frac{\pi}{2}(\delta+0.5)\right]}{\pi(\delta+0.5)} \tag{28}$$

By substitution of (26)∼(28) into the denominator of (22), the following expression is obtained

$$\begin{aligned}&(1-j)S_{0.5} - (1+j)S_{-0.5} + 2jS_0 \\ &\approx -j2Ae^{j\phi}e^{j\frac{\pi}{2}\delta}N\left[\frac{-\delta\cos(\pi\delta/2) + 0.5\sin(\pi\delta/2)}{\pi\delta(\delta+0.5)(\delta-0.5)}\right]\end{aligned} \tag{29}$$

By substitution of (29) into (22), the following expression is obtained

$$\begin{aligned}\hat{\delta} - \delta \approx \mathrm{Re}\Bigg\{ &\frac{je^{-j\phi-j\frac{\pi}{2}\delta}\left[\pi\delta(\delta+0.5)(\delta-0.5)\right]}{AN\left[\sin(\pi\delta/2) - 2\delta\cos(\pi\delta/2)\right]} \\ &\cdot\left[(1-j)(0.5-\delta)Z_{0.5} + (1+j)(0.5+\delta)Z_{-0.5} - 2j\delta Z_0\right]\Bigg\}\end{aligned} \tag{30}$$

So the MSE of the estimate of δ can be expressed as

$$\begin{aligned}E\left[\left(\hat{\delta}-\delta\right)^2\right] = \frac{1}{A^2N^2}\cdot\left[\frac{\pi\delta(\delta+0.5)(\delta-0.5)}{\sin(\pi\delta/2) - 2\delta\cos(\pi\delta/2)}\right]^2 \\ \cdot E\left(B^2\right)\end{aligned} \tag{31}$$

where

$$\begin{aligned}B = \mathrm{Re}\Big\{&je^{-j\phi-j\frac{\pi}{2}\delta}\left[(1-j)(0.5-\delta)Z_{0.5}\right. \\ &\left.+(1+j)(0.5+\delta)Z_{-0.5} - 2j\delta Z_0\right]\Big\}\end{aligned} \tag{32}$$

B can be expressed as

$$\begin{aligned}B = \mathrm{Re}\Big\{&je^{-j\frac{\pi}{2}\delta}\left[(1-j)(0.5-\delta)Z'_{0.5}\right. \\ &\left.+(1+j)(0.5+\delta)Z'_{-0.5} - 2j\delta Z'_0\right]\Big\}\end{aligned} \tag{33}$$

where $Z'_{0.5} = e^{-j\phi}Z_{0.5}$, $Z'_{-0.5} = e^{-j\phi}Z_{-0.5}$, $Z'_0 = e^{-j\phi}Z_0$.

Let $Z'_0 = U_0 + jV_0$, $Z'_{0.5} = U_{0.5} + jV_{0.5}$ and $Z'_{-0.5} = U_{-0.5} + jV_{-0.5}$. Then (33) can be expressed as

$$\begin{aligned}B = &\left[(0.5-\delta)(U_{0.5}+V_{0.5}) + (0.5+\delta)(U_{-0.5}-V_{-0.5})\right. \\ &\left.+2\delta V_0\right]\sin(\pi\delta/2) - \left[(\delta-0.5)(U_{0.5}-V_{0.5})\right. \\ &\left.+(0.5+\delta)(U_{-0.5}+V_{-0.5}) - 2\delta U_0\right]\cos(\pi\delta/2)\end{aligned} \tag{34}$$

As the intervals between the spectral lines X_0, $X_{0.5}$ and $X_{-0.5}$ used by the proposed estimator are smaller than Δf which is the frequency resolution of N-point FFT, the noise on different spectral lines are correlated. In order to compute $E\left(B^2\right)$, the correlation coefficients between X_0, $X_{0.5}$ and $X_{-0.5}$ are derived in the Appendix.

Using (34), (57), $E\left(U_{f_1}U_{f_2}\right) = E\left(U_{f_2}U_{f_1}\right)$, $E\left(V_{f_1}V_{f_2}\right) = E\left(V_{f_2}V_{f_1}\right)$, and $E\left(U_{f_1}V_{f_2}\right) = -E\left(U_{f_2}V_{f_1}\right)$, the following expression is obtained

$$\begin{aligned}E\left(B^2\right) \approx &\left(8\delta^2+1\right)E\left(U_0^2\right) - 8\delta^2E\left(U_0U_{0.5}\right) \\ &+(4\delta^2-1)E\left(U_{0.5}V_{-0.5}\right) + 8\delta^2E\left(U_0V_{0.5}\right)\end{aligned} \tag{35}$$

Zero-padding is performed before the $2N$-point FFT of the sinusoid sampled data. Therefore, the frequency interval between X_0 and $X_{0.5}$ is $-0.25/T$, the frequency interval between X_0 and $X_{-0.5}$ is $0.25/T$, and the frequency interval between $X_{0.5}$ and $X_{-0.5}$ is $0.5/T$. According to (55) and (60), the following expressions are obtained

$$E\left(U_0U_{0.5}\right) \approx N\sigma^2/\pi \tag{36}$$

$$E\left(U_0V_{0.5}\right) \approx -N\sigma^2/\pi \tag{37}$$

$$E\left(U_{0.5}V_{-0.5}\right) \approx -N\sigma^2/\pi \tag{38}$$

By substitution of (36)∼(38) into (35), (35) can be expressed as

$$E\left(B^2\right) \approx \left(8\delta^2+1\right)\frac{N\sigma^2}{2} - \left(12\delta^2+1\right)\frac{N\sigma^2}{\pi} \tag{39}$$

By substitution of (39) into (31), the following expression is obtained

$$\begin{aligned}E\left[\left(\hat{\delta}-\delta\right)^2\right] \approx &\frac{\pi^2\left(4\delta^2+0.5\right) - \pi\left(12\delta^2+1\right)}{4N\cdot SNR} \\ &\cdot\left[\frac{\delta(\delta+0.5)(\delta-0.5)}{\delta\cos(\pi\delta/2) - 0.5\sin(\pi\delta/2)}\right]^2\end{aligned} \tag{40}$$

When $\delta = 0$ and $\delta = \pm 0.5$, the numerator and the denominator of the above formula are all zero. The limit of the above formula can be calculated to obtain the values of $E\left[(\hat{\delta}-\delta)^2\right]$ when $\delta = 0$ and $\delta = \pm 0.5$. Therefore, the MSE of the estimate of δ can be expressed as

$$\begin{aligned}&E\left[\left(\hat{\delta}-\delta\right)^2\right] \\ &\approx \begin{cases}\dfrac{\pi^2\left(4\delta^2+0.5\right) - \pi\left(12\delta^2+1\right)}{4N\cdot SNR} \\ \cdot\left[\dfrac{\delta(\delta+0.5)(\delta-0.5)}{\delta\cos(\pi\delta/2) - 0.5\sin(\pi\delta/2)}\right]^2, \delta \neq 0, \pm 0.5 \\ \pi(\pi-2)/\left[8(4-\pi)^2N\cdot SNR\right], \delta = 0 \\ \pi(3\pi-8)/\left[4(\pi-2)^2N\cdot SNR\right], \delta = \pm 0.5\end{cases}\end{aligned} \tag{41}$$

IV. EXPERIMENTAL RESULTS

Computer simulations were performed to verify the performance of the algorithm presented above and the MSE calculation formula. The parameters used in the experiments of this section are as follows: $A = 1, f_0 = (N/4+\delta)f_s/N$, for example, $f_s = 512$kHz, $N = 512$, then $f = (128+\delta)$kHz $= 127.5 \sim 128.5$kHz, and the initial phase φ is uniformly distributed between 0 and 2π.The CRLB of mean square error (MSE) is [1]:

$$\mathrm{CRLB} = \frac{3f_s^2}{2\pi^2N(N^2-1)\cdot SNR} \tag{42}$$

Fig.1 shows the simulated RMSE of the proposed algorithm, Fang algorithm [8], RCTSL algorithm [9], AM algorithm [10], Djukanovic algorithm 1 [13] and Djukanovic algorithm 2 [14]. The presented algorithm, Fang algorithm and RCTSL algorithm are based on zero-padding and $2N$-point FFT. AM algorithm, Djukanovic algorithm 1 and Djukanovic algorithm 2 are without zero-padding and

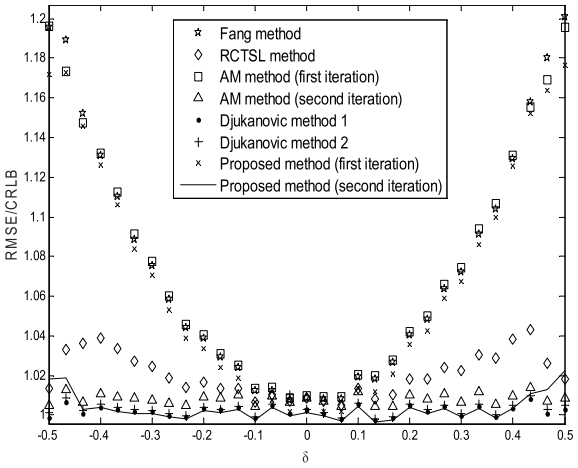

FIGURE 1. Simulated RMSE versus δ ($N = 512$, $SNR = 0$ dB).

TABLE 2. Numerical complexity of different algorithms.

Algorithm	Complex multiplications	Complex additions
Proposed (iteration 1)	$N\cdot\log_2(2N)+2N+4$	$2N\cdot\log_2(2N)+2N+1$
Proposed (iteration 2)	$N\cdot\log_2(2N)+5N+8$	$2N\cdot\log_2(2N)+5N+1$
AM [10] (iteration 1)	$(N/2)\cdot\log_2 N+2N+1$	$N\cdot\log_2 N+2N$
AM [10] (iteration 2)	$(N/2)\cdot\log_2 N+4N+2$	$N\cdot\log_2 N+4N$
Fang [8]	$N\cdot\log_2(2N)$	$2N\cdot\log_2(2N)$
RCTSL [9]	$N\cdot\log_2(2N)+1$	$2N\cdot\log_2(2N)$
Candan [6]	$(N/2)\cdot\log_2 N+1$	$N\cdot\log_2 N+3$
Djukanovic 1 [13]	$(N/2)\cdot\log_2 N+3N+1$	$N\cdot\log_2 N+3N$
Djukanovic 2 [14]	$(N/2)\cdot\log_2 N+2N+1$	$N\cdot\log_2 N+2N+1$

based on N-point FFT. We chose $N = 512$ and $SNR = 0$dB. δ is the residual frequency when $2N$-point FFT is performed. It can be seen that when δ varies from -0.5 to 0.5, the RMSE of the presented algorithm in the first iteration increases with the increase of $|\delta|$. When $|\delta|$ approaches zero, the RMSE of the presented algorithm approaches its minimum and is pretty close to CRLB. In the second iteration, the RMSE of the presented algorithm is pretty close to CRLB in the whole value range of δ and is lower than the RMSE of other methods (except for the case when $|\delta|$ is very close to 0.5). When $|\delta|$ is close to 0.5, the RMSE of RCTSL algorithm and Fang algorithm are relatively large (except for the algorithms in the first iteration). The reason is that under this circumstance, the amplitude of one neighbor of the maximum FFT spectrum line is close to its minimum, and is vulnerable to the noise.

The analytical and simulated RMSE of the presented algorithm are shown in Fig.2 for $SNR = 10$dB. And the values of N are 256 and 32 separately. In the first iteration, the theoretical RMSE is obtained according to (41). It can be seen that the theoretical calculation results are in good agreement with

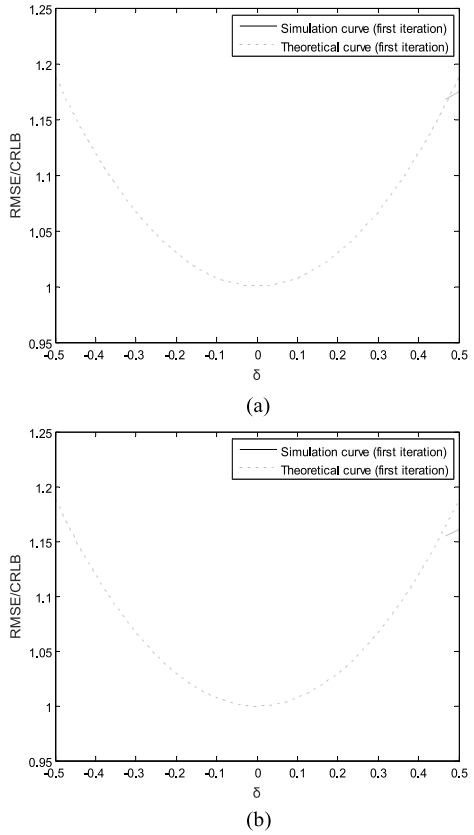

FIGURE 2. Analytical and simulated RMSE of the proposed algorithm ($SNR = 10$ dB): (a) $N = 256$ and (b) $N = 32$.

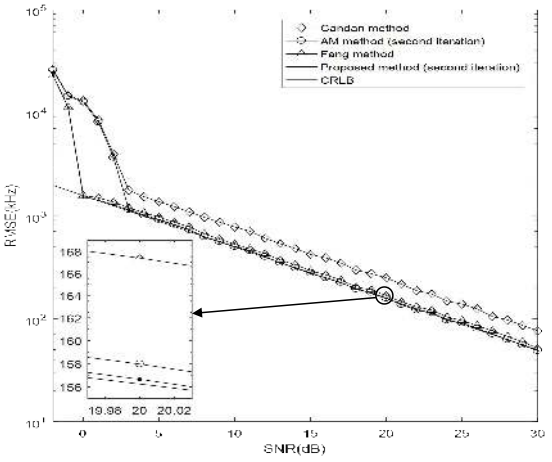

FIGURE 3. Simulated RMSE of Candan algorithm, AM algorithm, Fang algorithm and the proposed algorithm versus SNR ($N = 16$).

the simulation results. The RMSE of the presented algorithm increases as $|\delta|$ increases in the first iteration. When $|\delta|$ approaches zero, the RMSE of the presented algorithm is pretty close to CRLB.

Fig.3 and Fig.4 present the RMSE versus SNR of the proposed algorithm, Candan algorithm [6], AM algorithm [10], Fang algorithm [8], RCTSL algorithm [9], Djukanovic

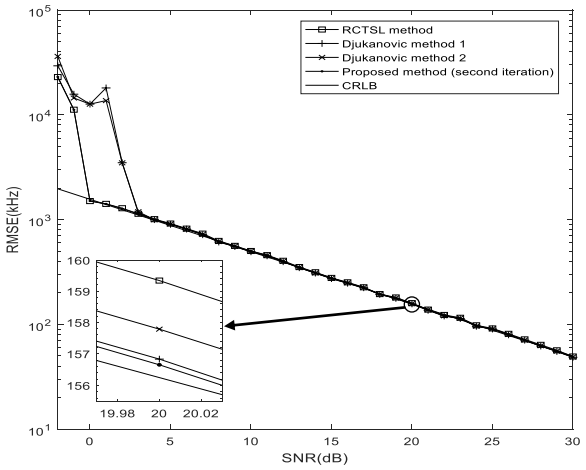

FIGURE 4. Simulated RMSE of RCTSL algorithm, Djukanovic algorithm 1, Djukanovic algorithm 2 and the proposed algorithm versus SNR ($N = 16$).

algorithm 1 [13] and Djukanovic algorithm 2 [14] for $N = 16$. δ obeys uniform distribution from -0.5 to 0.5. It can be seen that the SNR threshold of the presented algorithm is lower than that of Candan algorithm, Djukanovic algorithm 1, Djukanovic algorithm 2 and AM algorithm, and is identical to that of RCTSL algorithm and Fang algorithm. It can also be seen that the RMSE of the presented algorithm is lower than the RMSE of the other algorithms. The RMSE of Candan algorithm is obviously higher than that of the other algorithms.

TABLE 2 shows the numerical complexity of different algorithms. It can be seen that the presented algorithm in the second iteration has a bit higher computational complexity than that of Fang algorithm and RCTSL algorithm which are also based on $2N$-point FFT. Some additional computational effort is needed for the presented algorithm to achieve more accurate results and lower SNR threshold.

V. CONCLUSION

An accurate sinusoidal frequency estimation algorithm based on interpolation of FFT and DTFT is proposed in this paper. Zero-padding is performed before the FFT of the sinusoid sampled data. The fine estimate is obtained by employing the maximum FFT spectrum line and two DTFT sample values of the sinusoid located on the left and right side of the maximum FFT spectrum line. The correlation coefficients between the Fourier Transform of the noises on two arbitrarily spaced spectrum lines are derived. With these correlation coefficients, the MSE calculation formula is derived in additive white noise. The results of theoretical analysis and simulation show that the proposed estimator has lower RMSE than the competing FFT interpolation based estimators. The SNR threshold of the presented algorithm is lower than that of Candan algorithm, AM algorithm and Djukanovic algorithms. Although some additional computational effort is required to perform $2N$-point FFT and calculate the DTFT sample values, the presented algorithm is more accurate and its SNR threshold is lower.

APPENDIX

The correlation coefficients between the Fourier Transform of the noises on two arbitrarily spaced spectrum lines.

According to the DTFT definition, the DTFT of $z(n)$ at the location f is

$$Z_f = \sum_{n=0}^{N-1} z(n) \mathrm{e}^{-\mathrm{j}2\pi fTn/N} \tag{43}$$

Let $Z'_f = \mathrm{e}^{-\mathrm{j}\phi} Z_f$, the following expression is obtained

$$Z'_f = \sum_{n=0}^{N-1} z'(n) \mathrm{e}^{-\mathrm{j}2\pi fTn/N} \tag{44}$$

where

$$z'(n) = \mathrm{e}^{-\mathrm{j}\phi} z(n) \tag{45}$$

$z'(n)$ can be expressed as

$$z'(n) = z'_r(n) + \mathrm{j}z'_i(n) \tag{46}$$

$z'_r(n)$ is the real part of $z'(n)$, and $z'_i(n)$ is the imaginary part of $z'(n)$. Obviously $z'(n)$ has the same property with $z(n)$. The following expressions are obtained

$$E\left(z'_r(n)\right) = E\left(z'_i(n)\right) = E\left(z'(n)\right) = 0 \tag{47}$$

$$var\left(z'_r(n)\right) = var\left(z'_i(n)\right) = \frac{\sigma^2}{2} \tag{48}$$

$$E\left(z'_i(n) \cdot z'_i(m)\right) = E\left(z'_r(n) \cdot z'_r(m)\right) = \begin{cases} \frac{1}{2}\sigma^2, & n = m \\ 0, & n \neq m \end{cases} \tag{49}$$

$$E\left(z'_r(n) \cdot z'_i(m)\right) = 0 \tag{50}$$

Using U_f and V_f to represent the real part and the imaginary part of Z'_f, the following expressions are obtained

$$U_f = \sum_{n=0}^{N-1} \left[z'_r(n)\cos\left(2\pi fTn/N\right) + z'_i(n)\sin\left(2\pi fTn/N\right)\right] \tag{51}$$

$$V_f = \sum_{n=0}^{N-1} \left[-z'_r(n)\sin\left(2\pi fTn/N\right) + z'_i(n)\cos\left(2\pi fTn/N\right)\right] \tag{52}$$

The autocorrelation function of U_f at the location f_1 and f_2 which are near $m\Delta f$ is

$$\begin{aligned} &E\left(U_{f_1} U_{f_2}\right) \\ &= E\left\{\sum_{n=0}^{N-1} \left[z'_r(n)\cos\left(2\pi f_1 Tn/N\right) + z'_i(n)\sin\left(2\pi f_1 Tn/N\right)\right]\right. \\ &\quad \left. \cdot \sum_{m=0}^{N-1} \left[z'_r(m)\cos\left(2\pi f_2 Tm/N\right) + z'_i(m)\sin\left(2\pi f_2 Tm/N\right)\right]\right\} \end{aligned} \tag{53}$$

By substitution of (49) and (50) into (53), the following expression is obtained

$$\begin{aligned} &E\left(U_{f_1}U_{f_2}\right) \\ &= \frac{\sigma^2}{2}\sum_{n=0}^{N-1}\left[\cos\left(2\pi(f_1-f_2)Tn/N\right)\right] \\ &= \frac{\sigma^2\cdot\sin\left(\pi(f_1-f_2)T\right)}{2\sin\left(\pi(f_1-f_2)T/N\right)}\cdot\cos\left[\pi T(f_1-f_2)\left(1-\frac{1}{N}\right)\right] \end{aligned} \tag{54}$$

When N is large, the following expression is obtained

$$E\left(U_{f_1}U_{f_2}\right) \approx \frac{N\sigma^2\sin\left(2\pi(f_1-f_2)T\right)}{4\pi(f_1-f_2)T} \tag{55}$$

After similar derivation, the autocorrelation function of V_f is

$$\begin{aligned} &E\left(V_{f_1}V_{f_2}\right) \\ &= E\left\{\sum_{n=0}^{N-1}\left[-z_r'(n)\sin\left(\frac{2\pi f_1 Tn}{N}\right)+z_i'(n)\cos\left(\frac{2\pi f_1 Tn}{N}\right)\right]\right. \\ &\quad\left.\cdot\sum_{m=0}^{N-1}\left[-z_r'(m)\sin\left(\frac{2\pi f_2 Tm}{N}\right)+z_i'(m)\cos\left(\frac{2\pi f_2 Tm}{N}\right)\right]\right\} \\ &= \frac{\sigma^2}{2}\sum_{n=0}^{N-1}\left[\cos\left(\frac{2\pi f_1 Tn}{N}\right)\cos\left(\frac{2\pi f_2 Tn}{N}\right)\right. \\ &\quad\left.+\sin\left(\frac{2\pi f_1 Tn}{N}\right)\sin\left(\frac{2\pi f_2 Tn}{N}\right)\right] \end{aligned} \tag{56}$$

Formula (56) is the same with the first line of (54). Therefore, the following expression is obtained

$$E\left(V_{f_1}V_{f_2}\right) = E\left(U_{f_1}U_{f_2}\right) \tag{57}$$

The cross correlation function between U_f and V_f is

$$\begin{aligned} &E\left(U_{f_1}V_{f_2}\right) \\ &= E\left\{\sum_{n=0}^{N-1}\left[z_r'(n)\cos\left(2\pi f_1 Tn/N\right)+z_i'(n)\sin\left(2\pi f_1 Tn/N\right)\right]\right. \\ &\quad\left.\cdot\sum_{m=0}^{N-1}\left[-z_r'(m)\sin\left(2\pi f_2 Tm/N\right)+z_i'(m)\cos\left(2\pi f_2 Tm/N\right)\right]\right\} \end{aligned} \tag{58}$$

By substitution of (49) and (50) into (58), the following expression is obtained

$$\begin{aligned} E\left(U_{f_1}V_{f_2}\right) &= \frac{\sigma^2}{2}\sum_{n=0}^{N-1}\left[\sin\left(\frac{2\pi f_1 Tn}{N}\right)\cos\left(\frac{2\pi f_2 Tn}{N}\right)\right. \\ &\quad\left.-\cos\left(\frac{2\pi f_1 Tn}{N}\right)\sin\left(\frac{2\pi f_2 Tn}{N}\right)\right] \\ &= \frac{\sigma^2}{2}\sum_{n=0}^{N-1}\left[\sin\left(2\pi(f_1-f_2)Tn/N\right)\right] \\ &= \frac{\sigma^2}{2}\cdot\frac{\sin\left(\pi(f_1-f_2)T\right)}{\sin\left(\pi(f_1-f_2)T/N\right)}\sin\left[\pi T(f_1-f_2)\right. \\ &\quad\left.\times\left(1-\frac{1}{N}\right)\right] \end{aligned} \tag{59}$$

When N is large, the following expression is obtained

$$E\left(U_{f_1}V_{f_2}\right) \approx \frac{N\sigma^2\sin^2\left(\pi(f_1-f_2)T\right)}{2\pi(f_1-f_2)T} \tag{60}$$

REFERENCES

[1] D. Rife and R. Boorstyn, "Single tone parameter estimation from discrete-time observations," *IEEE Trans. Inf. Theory*, vol. 20, no. 5, pp. 591–598, Sep. 1974.

[2] A. J. S. Dutra, J. F. L. de Oliveira, T. de M. Prego, S. L. Netto, and E. A. B. da Silva, "High-precision frequency estimation of real sinusoids with reduced computational complexity using a model-based matched-spectrum approach," *Digit. Signal Process.*, vol. 34, pp. 67–73, Nov. 2014.

[3] Y.-Q. Tu and Y.-L. Shen, "Phase correction autocorrelation-based frequency estimation method for sinusoidal signal," *Signal Process.*, vol. 130, pp. 183–189, Jan. 2017.

[4] D. C. Rife and G. A. Vincent, "Use of the discrete Fourier transform in the measurement of frequencies and levels of tones," *Bell Syst. Tech. J.*, vol. 49, no. 2, pp. 197–228, Jul. 2013.

[5] V. K. Jain, W. L. Collins, and D. C. Davis, "High-accuracy analog measurements via interpolated FFT," *IEEE Trans. Instrum. Meas.*, vol. 28, no. 2, pp. 113–122, Jun. 1979.

[6] Ç. Candan,"A method for fine resolution frequency estimation from three DFT samples," *IEEE Signal Process. Lett.*, vol. 18, no. 6, pp. 351–354, Jun. 2011.

[7] C. Candan,"Analysis and further improvement of fine resolution frequency estimation method from three DFT samples," *IEEE Signal Process. Lett.*, vol. 20, no. 9, pp. 913–916, Sep. 2013.

[8] L. Fang, D. Duan, and L. Yang, "A new DFT-based frequency estimator for single-tone complex sinusoidal signals," in *Proc. MILCOM - IEEE Mil. Commun. Conf.*, Oct. 2012, pp. 1–6.

[9] C. Yang and G. Wei, "A noniterative frequency estimator with rational combination of three spectrum lines," *IEEE Trans. Signal Process.*, vol. 59, no. 10, pp. 5065–5070, Oct. 2011.

[10] E. Aboutanios and B. Mulgrew, "Iterative frequency estimation by interpolation on Fourier coefficients," *IEEE Trans. Signal Process.*, vol. 53, no. 4, pp. 1237–1242, Apr. 2005.

[11] J.-R. Liao and C.-M. Chen, "Phase correction of discrete Fourier transform coefficients to reduce frequency estimation bias of single tone complex sinusoid," *Signal Process.*, vol. 94, pp. 108–117, Jan. 2014.

[12] U. Orguner and Ç. Candan, "A fine-resolution frequency estimator using an arbitrary number of DFT coefficients," *Signal Process.*, vol. 105, pp. 17–21, Dec. 2014.

[13] S. Djukanovic, T. Popovic, and A. Mitrovic, "Precise sinusoid frequency estimation based on parabolic interpolation," in *Proc. 24th Telecommun. Forum (TELFOR)*, Nov. 2016, pp. 1–4.

[14] S. Djukanovic, "Sinusoid frequency estimator with parabolic interpolation of periodogram peak," in *Proc. 40th Int. Conf. Telecommun. Signal Process. (TSP)*, Jul. 2017, pp. 470–473.

[15] L. Fan and G. Qi, "A new synthetic frequency estimation method of sinusoid based on interpolated FFT," in *Proc. 5th Int. Conf. Instrum. Meas., Comput., Commun. Control (IMCCC)*, Sep. 2015, pp. 1725–1729.

[16] L. Fan, G. Qi, and W. He, "Accurate estimation method of sinusoidal frequency based on FFT," in *Proc. 35th Chin. Control Conf. (CCC)*, Jul. 2016, pp. 5164–5167.

[17] L. Fan and G. Qi, "Frequency estimator of sinusoid based on interpolation of three DFT spectral lines," *Signal Process.*, vol. 144, pp. 52–60, Mar. 2018.

[18] S. Djukanovic and V. Popovic-Bugarin, "Efficient and accurate detection and frequency estimation of multiple sinusoids," *IEEE Access*, vol. 7, pp. 1118–1125, 2019.

[19] A. Serbes, "Fast and efficient sinusoidal frequency estimation by using the DFT coefficients," *IEEE Trans. Commun.*, vol. 67, no. 3, pp. 2333–2342, Mar. 2019.

[20] Ç. Candan,"Fine resolution frequency estimation from three DFT samples: Case of windowed data," *Signal Process.*, vol. 114, pp. 245–250, Sep. 2015.

[21] D. Belega and D. Petri, "Frequency estimation by two- or three-point interpolated Fourier algorithms based on cosine windows," *Signal Process.*, vol. 117, pp. 115–125, Dec. 2015.

[22] D. Belega, D. Petri, and D. Dallet, "Impact of harmonics on the interpolated DFT frequency estimator," *Mech. Syst. Signal Process.*, vols. 66–67, pp. 349–360, Jan. 2016.

[23] D. Belega and D. Petri, "Effect of noise and harmonics on sine-wave frequency estimation by interpolated DFT algorithms based on few observed cycles," *Signal Process.*, vol. 140, pp. 207–218, Nov. 2017.
[24] Y. Wang, W. Wei, and J. Xiang, "Multipoint interpolated DFT for sine waves in short records with DC components," *Signal Process.*, vol. 131, pp. 161–170, Feb. 2017.
[25] S. Djukanovic, "An accurate method for frequency estimation of a real sinusoid," *IEEE Signal Process. Lett.*, vol. 23, no. 7, pp. 915–918, Jul. 2016.
[26] D. Belega and D. Petri, "Influence of the noise on DFT-based sine-wave frequency and amplitude estimators," *Measurement*, vol. 137, pp. 527–534, Apr. 2019.
[27] D. Belega, D. Petri, and D. Dallet, "Accurate frequency estimation of a noisy sine-wave by means of an interpolated discrete-time Fourier transform algorithm," *Measurement*, vol. 116, pp. 685–691, Feb. 2018.
[28] H. Wen, C. Li, and W. Yao, "Power system frequency estimation of sine-wave corrupted with noise by windowed three-point interpolated DFT," *IEEE Trans. Smart Grid*, vol. 9, no. 5, pp. 5163–5172, Sep. 2018.

LEI FAN was born in 1980. He received the B.Sc., M.Sc., and Ph.D. degrees in information and communication engineering from Dalian Maritime University, in 2003, 2006, and 2018, respectively. He is currently a Lecturer with the School of Information Science and Engineering, Dalian Polytechnic University, China. His research interests include parameter estimation, signal detection, and signal processing.

GUOQING QI was born in 1960. He received the B.Eng. degree in electronic engineering from the Dalian University of Science and Technology, in 1982, and the M.Eng. degree in radio navigation technology and Ph.D. degree in marine engineering from Dalian Maritime University, China, in 1984 and 2001, respectively. He is currently a Professor with the School of Information Science and Technology, Dalian Maritime University. His research interests include digital signal processing, image processing, and radar signal processing.

JUN XING was born in 1972. He received the B.Sc. and M.Sc. degrees in computer technology and application from Northeastern University, in 1996 and 1999, respectively, and the Ph.D. degree in computer technology and application from the Dalian University of Technology, in 2008. He is currently a Lecturer with the School of Information Science and Engineering, Dalian Polytechnic University, China. His research interests include the Internet of Things and large data algorithms.

JIYU JIN received the Ph.D. degree in information and communication engineering from Yeungnam University, Gyeongsan, South Korea, in 2007. From 2007 to 2008, he was a Postdoctoral Researcher with the School of Electrical Engineering and Computer Science, Seoul National University, South Korea. From 2008 to 2009, he was an Assistant Professor of information and communication engineering with Yeungnam University. He joined Hilandwe Communication Technology Company Ltd., as a Technical Director, in 2010. He is currently an Associate Professor with the School of Information Science and Engineering, Dalian Polytechnic University, China. His research interests include wireless/mobile communication systems, the Internet of Things, and deep learning.

JINYU LIU is currently pursuing the bachelor's degree in communication engineering with Dalian Polytechnic University (DLPU), China. He is a member of the Research and Development Institute of Integrated Measurement and Control, DLPU. His research interests include signal detection and parameter estimation.

ZHISEN WANG received the Ph.D. degree from the Electrical and Communication Engineering Department, National Northeast University, Japan, in 2007. He is currently a Professor with the School of Information Science and Engineering, Dalian Polytechnic University (DLPU), China. He is also the Director of the Research and Development Institute of Integrated Measurement and Control, DLPU. His research interests include wireless communication and networks, digital signal processing, the IoT theory, and the IoT technology.